INTEGRAL BEHAVIOR OF THE ATLAS FACILITY FOR A 3-INCH SMALL BREAK LOSS OF COOLANT ACCIDENT

KI-YONG CHOI*, HYUN-SIK PARK, SEOK CHO, DONG-JIN EUH, YEON-SIK KIM and WON-PIL BAEK
Thermal Hydraulics Safety Research Division, Korea Atomic Energy Research Institute
1045 Daedeokdaero, Yuseong-gu, Daejeon 305-353, Korea
*Corresponding author. E-mail : kychoi@kaeri.re.kr

Received November 21, 2007
Accepted for Publication January 31, 2008

A small-break loss of coolant accident (SB-LOCA) test with a break size equivalent to a 3-inch cold leg break of the APR1400 was carried out as the first transient integral effect test using the ATLAS (Advanced Thermal-hydraulic Test Loop for Accident Simulation). This was the first integral effect test to investigate the integral performance of the test facility and to verify its simulation capability for one of the design-basis accidents. Reasonably good thermal hydraulic data was obtained so that an integral performance of the fluid sub-systems was identified and control performance of the ATLAS was confirmed under real thermal hydraulic conditions. Based on the measured data, a post-test calculation was carried out using the best-estimate thermal hydraulic safety analysis code, MARS 3.1, and the similarity between the expected and actual data was investigated. On the whole, the post-test calculation reasonably predicts the major thermal hydraulic parameters measured during the SB-LOCA test. The obtained data will be used to enhance the simulation capability of the ATLAS and to improve an input model of the ATLAS for simulation of other target scenarios.

KEYWORDS : APR1400, ATLAS, SBLOCA, Thermal-Hydraulics

1. INTRODUCTION

1.1 Background

Over the past 30 years, several large integral facilities have been utilized in order to understand transient behavior in nuclear power plants. The main objective of these integral facilities was to enhance our physical understanding of transient phenomena during LOCA or non-LOCA transients. An integral database was also used as a basis for the development and verification of thermal hydraulic safety analysis codes. A comprehensive literature survey on the world's integral facilities can be found in the literature [1]. The important scaling features of these integral facilities and their major test items are summarized in Table 1. All these facilities were scaled down with respect to the reference plant by optimizing the costs and benefits. Most of them have a full height scale and a reduced volume scale. Each integral facility was established to reflect the design features specific to its reference plant and to focus on a certain thermal hydraulic phenomena. The integral test items were limited by the system configuration and the simulation capability of a facility.

In Korea, the SNUF (Seoul National University integral test Facility) was the first attempt to carry out integral tests of nuclear plants for design basis accidents (DBAs). It aimed at a simulation of a large-break LOCA (LB-LOCA) and a direct vessel injection (DVI) line break under reduced pressure conditions [2, 3]. However, the SNUF is a small facility which is operated at reduced pressure conditions as compared with other facilities. It has a limited simulation capability for major event scenarios due to low core power and the fact that the secondary system is simplified as a lumped boundary condition. Recently, KAERI launched a large-scale integral effect test program sponsored by the Korean government and finished constructing a test loop, the ATLAS, at the end of 2005 [4]. The reference plant for the ATLAS is the APR1400, which is an advanced power reactor developed by Korean industry. The ATLAS was designed to have the capability of simulating manifold scenarios, including the reflood phase of the LB-LOCA, SB-LOCA scenarios including a DVI line break, a steam generator tube rupture, a steam or a feed line break, and a mid-loop operation, etc. The ATLAS has a particular focus on the reproduction of the multi-dimensional phenomena related to a DVI as well as on preservation of the surface tension effect and the flow regime in the design stage of the reactor vessel and downcomer. Accordingly, the ATLAS adopted an integrated annulus downcomer which is the

Table 1. Summary of the World's Major Integral Facilities

Country	Facility	Reference plant	Volume scale	Height scale	Press. (MPa)	Test items
USA	Semiscale	W 4L PWR	1/1706	1/1	15.5	SBLOCA, ECCS
	LOFT	Trojan 4L PWR	1/50	1/1, 1/2	15.5	LOCA, ECCS
	UMCP	B&W PWR	1/500	1/4.4	2.1	SBLOCA, Natural Cir.
	MIST	B&W PWR	1/817	1/1	15.0	SBLOCA, Natural Cir.
	APEX	W AP600	1/192	1/4	2.8	SBLOCA, ADS, CMT
	PUMA	GE-SBWR	1/400	1/4	1.0	LOCA, PCCS, GDCS
Japan	LSTF	W 4L PWR	1/48	1/1	16.0	SBLOCA, EOP, AMP
France	BETHSY	Fram. 3L PWR	1/100	1/1	17.2	SBLOCA, LBLOCA
Germany	PKL	KWU PWR	1/145	1/1	4.5	Refill & Reflood of LOCA
Italy	LOBI	KWU 4L PWR	1/700	1/1	15.0	SBLOCA, AMS, SBO, SG
	SPES	W AP600	1/395	1/1	20.0	SBLOCA, SGTR, SLB
Russia	PSV-VVER	VVER-1000	1/300	1/1	18.0	LBLOCA, SBLOCA, AMP
	KMS	VVER-640	1/27	1/1	18.0	LBLOCA, SBLOCA, AMP
Taiwan	IIST	W 3L PWR	1/400	1/4	2.1	EOP, PCCS for APWR
Korea	SNUF	APR1400	1/1139	1/6.4	0.8	LBLOCA, DVI line break
	ATLAS	APR1400	1/288	1/2	17.5	SBLOCA, LBLOCA, etc

same design feature present in the reference plant. The ALTAS also incorporates some specific design features of the Korean standard nuclear power plant, the OPR1000, such as a cold-leg injection mode for a safety injection and a low-pressure safety injection mode. The simulation capability of the ATLAS for major DBAs was studied with the best-estimate safety analysis code, MARS [5]. It was found that overall similarity between the reference plant and the ATLAS was acceptable.

The APR1400 features increased efficiency in the use of emergency core cooling (ECC) water by including a passive fluid device inside the safety injection tank (SIT). The fluidic device passively controls the discharge flow rate in the reactor vessel during refill and reflood phases by changing the flow resistance inside the vortex chamber of the fluidic device [6]. The advantages of the improved SIT are twofold: it can remove an excessive delivery of ECC water to the reactor vessel when the water level has been raised to the bottom of the cold leg, and the safety injection system can be simplified by eliminating the low pressure safety injection (LPSI) pumps. However, the elimination of LPSI pumps results in a situation where the ECC water flow is provided only by high pressure injection (HPSI) pumps after the SITs become empty in the late reflood phase of the LB-LOCA. A downcomer boiling, which is one of the results of releasing the stored energy in the vessel metal mass due to an insufficient ECC water flow, will degrade core cooling capability in two ways: reducing a subcooling of the coolant entering the core and by a loss of coolant mass out of the break due to boiling along the downcomer. The thermal hydraulics occurring in the downcomer region during the late reflood phase of the LB-LOCA thus became the most important safety issue for the APR1400 in terms of obtaining licensure from the Korean regulatory organization. Therefore, LB-LOCA tests will be performed intensively in the first phase of the ATLAS program.

1.2 Objectives

Since the establishment of the ATLAS, a series of preliminary tests have been carried out to identify the major thermal hydraulic characteristics of the system such as coolant inventory distribution, pressure drop, or temperature distribution along the primary loop. These preliminary

tests also included performance verification tests for the major active components comprising the ATLAS such as the core or pressurizer heaters, reactor coolant pumps, heat exchangers, instrumentations, and control or on-off valves. The major preliminary test results are summarized in a report [7].

Before the integral effect tests on LB-LOCAs were carried out in earnest, a preliminary integral effect test for an SB-LOCA at a cold leg was performed. The present test is named SB-CL-01. It is an SB-LOCA with a break size equivalent to a 3-inch cold leg break of the APR1400. The main purpose of this test was to investigate the thermal hydraulic response of the entire ATLAS system during the integral test and to verify the reliability of the instrumentation and control system. As the ATLAS consists of extensive components and sub-systems, the performance of each component or sub-system needs to be verified carefully to ensure a reliable integral test. Most performance tests can be conducted at a cold condition, whereas the performance of certain components such as heaters, pumps, and valves must be confirmed through an integral test under high pressure and temperature conditions. Furthermore, instrumentation designed to work under two-phase conditions should also be confirmed under real conditions.

Another objective of the present work is to improve the ATLAS model for the best estimate thermal hydraulic safety analysis code MARS 3.1[8]. Based on the measured transient data of SB-CL-01, a post-test calculation was also carried out with the same boundary conditions. The simulation capability of the MARS code for the SB-LOCA will be assessed by a comparison of the major thermal hydraulic parameters. The present ATLAS model for a MARS analysis is based on several assumptions which were determined from an ideal scaling. Obtained integral data will be used to improve the ATLAS model for a code calculation to predict thermal hydraulic phenomena with a minimum distortion.

2. DESCRIPTION OF THE ATLAS

2.1 Configuration of a Fluid System

The ATLAS has the same two-loop features as the APR1400 and is designed according to the well-known scaling method suggested by Ishii and Kataoka [9] to simulate the various test scenarios as realistically as possible. It is a half-height and 1/288 volume scaled test facility with respect to the APR1400. The main motive for adopting the reduced-height design is to allow for an integrated annular downcomer where multidimensional phenomena can be important in some accident conditions with a DVI operation. According to the scaling law, the reduced height scaling method results in time-reducing results in the model. For the one-half-height facility, the time for the scaled model is a square root 2 times faster than the prototypical time. The friction factors in the scaled model are maintained at the same values as those of the prototype. The hydraulic diameter of the scaled model is maintained the same as that of the prototype to preserve the prototypical conditions for the heat transfer coefficient. Major scaling parameters of the ATLAS are summarized in Table 2.

Table 2. Major Scaling Parameters of the ATLAS

Parameters	Scaling law	ATLAS design
Length	l_{oR}	1/2
Diameter	d_{oR}	1/12
Area	d^2_{oR}	1/144
Volume	$l_{oR}\, d^2_{oR}$	1/288
Core DT	DT_{oR}	1
Velocity	$l^{1/2}_{oR}$	1/1.414
Time	$l^{1/2}_{oR}$	1/1.414
Power/Volume	$l^{-1/2}_{oR}$	1.414
Heat flux	$l^{-1/2}_{oR}$	1.414
Core power	$l^{1/2}_{oR}\, d^2_{oR}$	1/203.6
Flow rate	$l^{1/2}_{oR}\, d^2_{oR}$	1/203.6
Pressure drop	l_{oR}	1/2

The fluid system of the ATLAS consists of a primary system, a secondary system, a safety injection system, a break simulation system, a containment simulation system, and several auxiliary systems. The primary system includes a reactor vessel, two hot legs, four cold legs, a pressurizer, four reactor coolant pumps (RCPs), and two steam generators. The secondary system of the ATLAS is simplified to a circulating loop-type. The steam generated by two steam generators is condensed in a direct condenser tank and the condensed feedwater is again injected to the steam generators. Most of the safety injection features of the APR1400 and the OPR1000 are incorporated into the safety injection system of the ATLAS. It consists of four safety injection tanks (SITs) and a high pressure injection (HPSI) pump which can simulate several operation modes such as charging, letdown, auxiliary spray, pre-heating, safety injection, long-term cooling, shutdown cooling, and recirculation operations. The break simulation system consists of a quick opening valve, a break nozzle and instruments. It is precisely manufactured to have a scaled break flow through it in the case of LOCA tests. The ATLAS containment simulation system has a function that collects the break flow rate and maintains a specified pressure in order to simulate containment. A separator in the containment

simulation system separates a liquid phase from a two-phase break flow and each separated flow rate in a single phase condition is measured by a different measuring technique. The separated liquid flow rate is measured by weighing a mass of accumulated water; the separated vapor flow rate is measured by a dedicated flowmeter. The ATLAS also features some auxiliary systems such as a makeup system, a component cooling system, a nitrogen/air/steam supply system, a vacuum system, and a heat tracing system. A three-dimensional view of the ATLAS is shown in Fig. 1. ATLAS design details and a description of the ATLAS development program can be found in the literature [4,10].

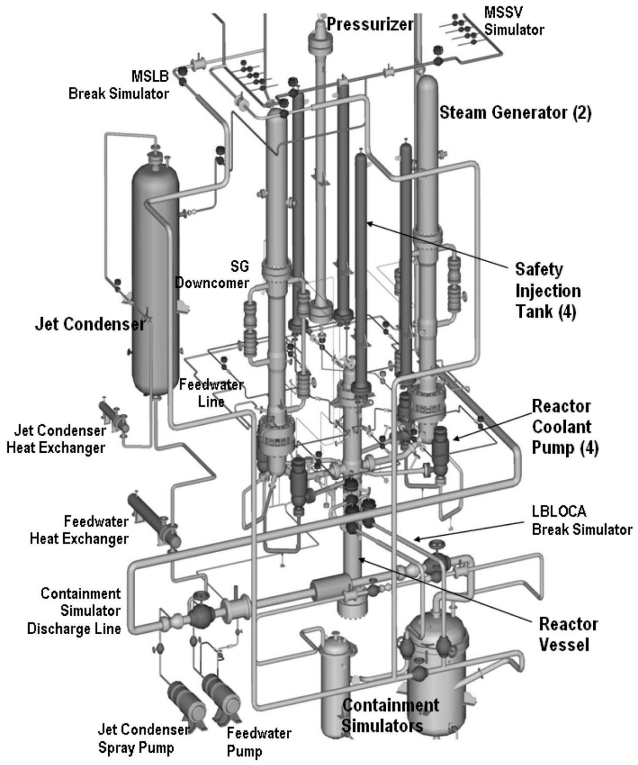

Fig. 1. Schematics of the Overall ATLAS

2.2 Configuration of a Control and Instrumentation System

The control and data acquisition system of the ATLAS was built with a hybrid distributed control system (DCS). The input and output modules are distributed into 10 cabinets and they are controlled by two CPUs. The raw signals from the field are processed or converted to engineering units (EU) in a system server and the processed or converted signals are monitored and controlled through the HMI (Human Machine Interface) system by operators. The ARIDES system, which operates on a LINUX platform, is used as control software. The IO signals include AI (Analog Input), AO (Analog Output), TC (Thermocouple), DI (Digital Input), DO (Digital Output), and SR (Serial communication). The total number of signals is 2010. In addition, there are about 1500 logically derived IO signals. All IO signals are processed at 10Hz. Instrument signals can also be categorized according to instrument type, such as temperature, static pressure, differential pressure, water level, flow rate, power, and rotational speed.

The HMI consists of 43 processing windows and they are classified according to the ATLAS fluid system. All the control devices can be controlled by a manual, auto, sequence, group, or table control method. The control logics are distributed in the RTP CPU, the system server and the HMI itself. The control logics which directly control or protect the control devices in the field are installed in the RTP CPU. Flexible control logics which control and monitor the sequential operations of the control devices are installed on the system server. They are based on a standard C++ program structure and can be easily customized according to user requests. Flexibility is essential for the implementation of major accident scenario simulations of the APR1400/OPR1000 using the ATLAS. Some control logics which are needed for the purpose of communication between the system server and the HMI are also installed at the HMI.

The monitoring system can display real-time trends or the historical data of the selected IO signals on LCD monitors in a graphical form. The data logging system can be started or stopped by operators and the logging frequency can be selected from among 0.5, 1, 2, and 10Hz. The raw signals as well as the EU-converted signals are saved in one of three operator processing stations. The ATLAS has a protection system which protects operators in the main control room and prevents the major hardware from failing in the case of an emergency. The protection system consists of a software protection that functions by control logics and a manual protection device on the main control room emergency panel. A detailed description of the ATLAS control system can be found in the literature [11].

3. MARS ANALYSIS

The MARS code is a best estimate safety analysis code developed by KAERI through unifying and restructuring the RELAP5/MOD3.2.1[12] and COBRA-TF [13]. The MARS code has the capability of analyzing a one-dimensional and three-dimensional thermal-hydraulic system as well as the fuel responses of light water reactor transients. The thermal hydraulic modeling capability of the MARS code has been continuously improved and extended for an

application not only to light and heavy water reactors but also to research reactors and to many advanced reactor types. Many other models and capabilities were added to the first version and the latest version of the series is the MARS 3.1. Notable upgrades include 3-dimensional simulation capabilities incorporated into the latest version in order to treat a turbulent mixing model and a conduction model. [8]

The one-dimensional model of the MARS 3.1 code was used for a pre-test and a post-test analysis of an SB-LOCA event. The pre-test analysis for an SB-LOCA at a cold leg of the APR1400 with a break size of 3 inches was done before the integral effect test was carried out. The main purpose of the pre-test analysis was to define the sequence of events (SOE) during the progression of the SB-LOCA event, which can be applied to the ATLAS. The obtained SOE can be found in Table 3.

Figure 2 shows a nodalization diagram for the present analysis. The same nodalization method was used both for the APR1400 and for the ATLAS system. All the detailed components of the ATLAS were modeled for the present analysis. All the reactor coolant systems including the reactor vessel, the primary piping, and the reactor coolant pumps were modeled based on the detailed design data of the ATLAS. As shown in Fig. 2, the annular section of the downcomer is modeled as 6 columns which are split azimuthally every 60°. These columns are also divided by 10 axial nodes, and are connected by a cross flow junction component in a circumferential direction to simulate the multi-dimensional flow behavior in a downcomer. One broken and three intact cold legs as well as 4 DVI lines are connected in the normal direction to the outer surface of the downcomer. There is still an argument over the nodalization method for the annulus downcomer region. No accepted method is available which can take account of the three-dimensional effects in the downcomer region using the one-dimensional components of the MARS code. The present treatment of the downcomer regions connecting circumferential volumes with cross flow junctions is based on a method in the literature [5]. It was found that the similarities between the APR1400 and ATLAS for the major DBAs were reasonable with the current nodalization method. The reactor coolant pumps were modeled with homologous data which was obtained from a separate performance test of the reactor coolant pumps installed in the ATLAS. A pressurizer is connected at the intact cold leg. As for the secondary system, two steam generators and main steam lines were modeled. A feedwater system and a turbine system were treated with

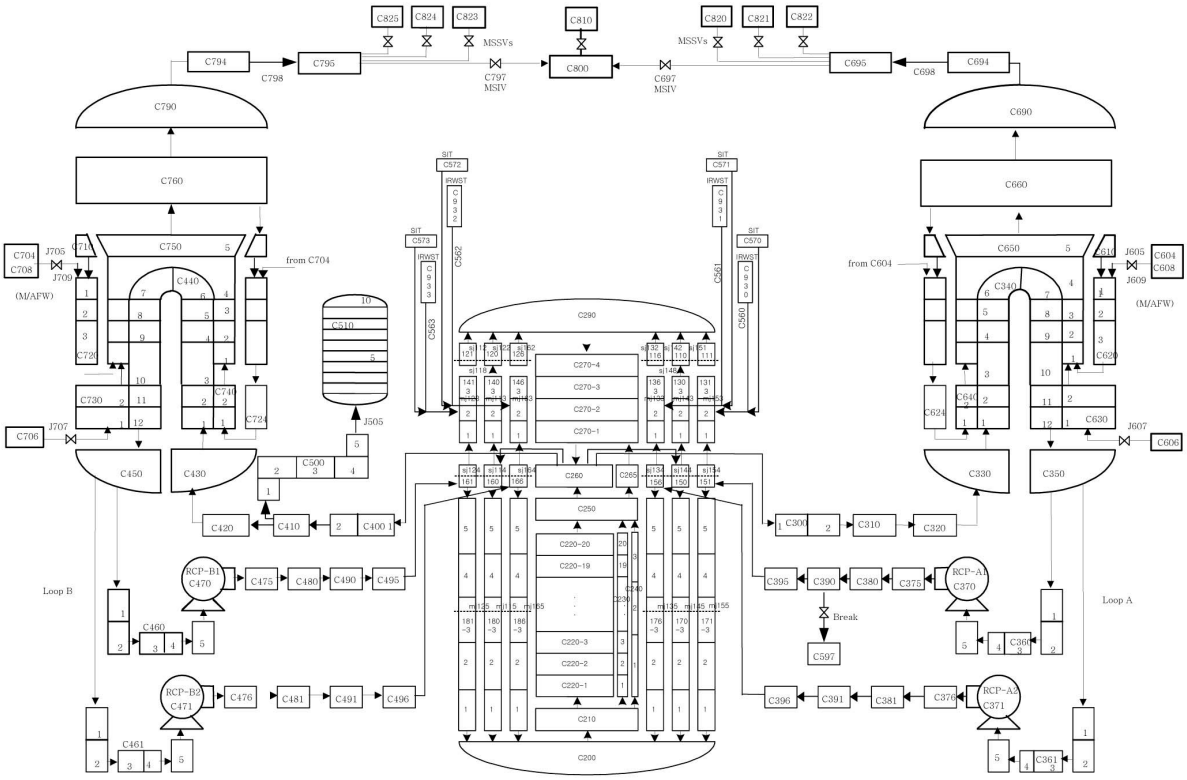

Fig. 2. MARS 1-D Nodalization for a Simulation of the SB-CL-01 Test

Table 3. Major Sequence of Events for the SB-CL-01 Test

Event	APR1400	ATLAS	Measured/Calculated time (sec)	Action (Control devices)
Break begins			150/150	- Opening of the break valve (OV-BS-06)
LPP[1)]	P_{pzr}<10.7214MPa	P_{pzr}<10.7214MPa	214/211.3	- LPP signal is generated based on the pressurizer pressure
Reactor trip	LPP + 1.15sec	LPP + 0.81sec	302.8/299.3	- Table controls of core heaters are initiated (HP-CO-01,02,03) *88 sec delay in test
Turbine trip	LPP + 0.14sec	LPP + 0.10sec	214.1/212.2	- Steam control valve is isolated (FCV-MSCV-01)
RCP trip	LPP + 0.5sec	LPP + 0.36sec	214.4/212.5	- All RCPs are tripped (PP-RCP1,2A,B-01)
MSIAS[2)]	Reactor trip + 10sec	Reactor trip + 7.07sec	221.9/219.6	- MSIA signal is generated with a time delay after the reactor trip
Steam generator isolation	MSIAS + 0sec	MSIAS + 0sec	221.9/219.6	- Feedwater control and steam isolation valves are isolated (FCV-MF1,2-01,02, OV-MSIV1,2-01)
HPSI begins	LPP + 40sec	LPP + 28.28sec	256/239.6	- Table control of the HPSI pump is initiated (PP-HPSI1,3-01) - Control and isolation valves are open (FCV-HPSI1,3-01, OV-SIS1,3-01) *13 sec delay in test in a pipeline
SIT[3)]	P_{DC} <4.03MPa	P_{DC} <4.03MPa	2983/3457.1	- SIT signal is generated based on the downcomer pressure
SIT begins	SIT + 0sec	SIT + 0sec	2983/3457.1	- Control and isolation valves are open (FCV-SIT1,2,3,4-01, OV-SIS2,4-01)

[1)] LPP : Low Pressurizer Pressure
[2)] MSIAS : Main Steam Isolation Actuation Signal
[3)] SIT : Safety Injection Tank Open Signal

a boundary condition, and were modeled by a time dependent volume component. The safety injection system was also modeled, including four SITs and four HPSI pumps. In the present analysis, a single failure assumption was applied so that four SITs and 2 of the 4 HPSI pumps were used during the transient.

After the SB-LOCA test was performed according to the SOE in Table 3, a post-test analysis was carried out to investigate the simulation capability of the MARS code with the obtained data. Table 4 shows a comparison of the major parameters when a system reaches a steady state condition. As can be seen in Table 4, most of the calculated parameters agree with the measured values. When a reasonable steady state condition was obtained, the transient calculation was restarted by initiating an SB-LOCA at a cold leg.

Table 4. Comparison of the Major Parameters at a Steady State Condition

Design Parameters	ATLAS	MARS3.1	Remarks
Case Description	Data	Calculation	
Reactor Vessel			
Normal Power, MWt	1.567	1.567	8% power
Pressurizer P., MPa	15.8	15.9	+0.1MPa
Pressurizer T., ºC	348.7	346.8	-1.9 ºC
Core Inlet .Temp., ºC	288.3	291.1	+2.8 ºC
Core Outlet .Temp., ºC	316.8	316.8	
Core Flow, kg/s	~10.1(est.)	10.6	+0.5 kg/s
Primary Piping			
Hot Leg Temp. ºC	317	316.5	-0.5 ºC
Cold Leg Temp. ºC	291	290.6	-0.4 ºC
Steam Generator			
Feedwater Flow Rate/SG, kg/s	~0.29	0.34	+0.05 kg/s
Steam Flow Rate/SG, kg/s	~0.29	0.34	
Feedwater Temperature, ºC	108	108	
Steam Pressure. MPa	8.0	7.4	-0.6 MPa
Steam Temp. ºC	294.5	289.5	-5.0 ºC

4. RESULTS AND ANALYSIS

4.1 Test Preparation

Several preparatory works were conducted in order to perform the SB-CL-01 test. As described in the previous section, the sequence of events for the SB-CL-01 test was determined based on the pre-test analysis results shown in Table 3. The sequence control logics used in the pre-test analysis for the APR1400 plants were applied to the present test. The delay time between successive sequence control signals was conserved according to the scaling law. As the time was reduced by a square root of two in the ATLAS system due to its half-height scale, delay time reduced by a square root of two was applied to the sequence control logics of the ATLAS. The detailed sequence of events is summarized in Table 3.

The control devices of the ATLAS were programmed to follow the events defined in Table 3 according to the control signals. Among the control devices, the core heaters and the HPSI pump were controlled by a predefined table. The core heater power was initially 8% of the scaled full power and it was programmed to then follow the decay power table. 120% of the ANS73 decay curve was used to generate the decay power table. The other important control device was the HPSI pump. In the APR1400, it is a centrifugal pump and the injected water flow rate depends on the system pressure. However, in the ATLAS, a metering -type injection pump was installed because it can easily supply the required HPSI flow rate. If a reciprocating speed is fixed for the HPSI pump, the discharged flow rate is independent of the discharge pressure. The relationship between the system pressure and the HPSI flow rate was first obtained from the pre-test calculation. It is a requirement that the HPSI pump delivers emergency water into the reactor pressure vessel according to the system pressure. The speed for the HPSI pump to provide the required HPSI flow rate was then obtained experimentally for a given position of the control valve that is installed between the HPSI pump and the reactor pressure vessel. Finally, a control table between the speed of the HPSI pump and the system pressure during the SB-LOCA transient was determined. The control table was thus programmed in order to deliver the required HPSI flow rate to the primary system of the ATLAS.

The other controls are related to a simple sequence of controls such as opening or closing valves and tripping RCPs. They were controlled by triggering signals which were generated when a certain measured signal was greater or smaller than a set valve.

4.2 Major Test Results

4.2.1 Break Flow Rate

Measured and calculated times for the major events during the SB-LOCA test are tabulated in Table 3. The test was started by quickly opening the break simulation valve OV-BS-06 when the system was judged to have reached a quasi-steady state. The break simulation system consists of a quick opening valve, a break nozzle, a case holding the break nozzle, and a few instruments. When an SB-LOCA occurs, a choking is expected to occur at the break location. Therefore the break area should be scaled down according to the scaling ratio of the flow rate, 1/203.6. The inner diameter of the break nozzle was determined to be 5.34mm, which corresponds to 1/203.6 of a 3-inch break area.

The break flow was discharged through a break simulation nozzle to a containment simulation system, which consisted of two separating vessels and five measuring vessels to incorporate a broad break flow rate, depending on the target scenarios as shown in Fig. 3. In the present SB-CL-01 test, only one separating vessel was used because the break flow rate was expected to be small. The break nozzle was installed vertically downward at the bottom of the broken cold leg. The break flow from the broken cold leg was collected into the separating vessel, SV-01. The separated steam in the separating vessel was discharged through a silencer to the atmosphere. The steam flow rate was measured by a vortex-type flow meter at the discharge line. The separated water in the separating vessel was drained to one of the five measuring vessels. A load cell was installed on the bottom of each measuring vessel to weigh the water mass. In the present test, two measuring vessels, MV-01 and MV-02, were alternatively used to weigh the drained water mass. First the separated water was introduced to the MV-01. When MV-01 was full of water, the flow direction was switched from MV-01 to MV-02 through a 3-way valve. When the MV-02 was used to measure the water mass, the MV-01 was drained for the next usage and vice versa. The measured variation of the water mass is shown in Fig. 4 where alternatively varying trends of an accumulating water mass can be seen. The mass change rate with respect to time was converted to a mass flow rate and is plotted in Fig. 5 together with a measured steam flow rate. The total break flow rate was calculated by a summation of the water and steam flow rate. The water flow rate shows a severe fluctuation when compared with the measured steam flow rate. It seems that the uncertainty in measuring a water mass by a load cell needs to be improved. Figure 5 also shows the calculated total break flow rate according to the MARS code. It is shown that the calculated rate agrees with the measured data well.

The separating vessel was also designed to simulate

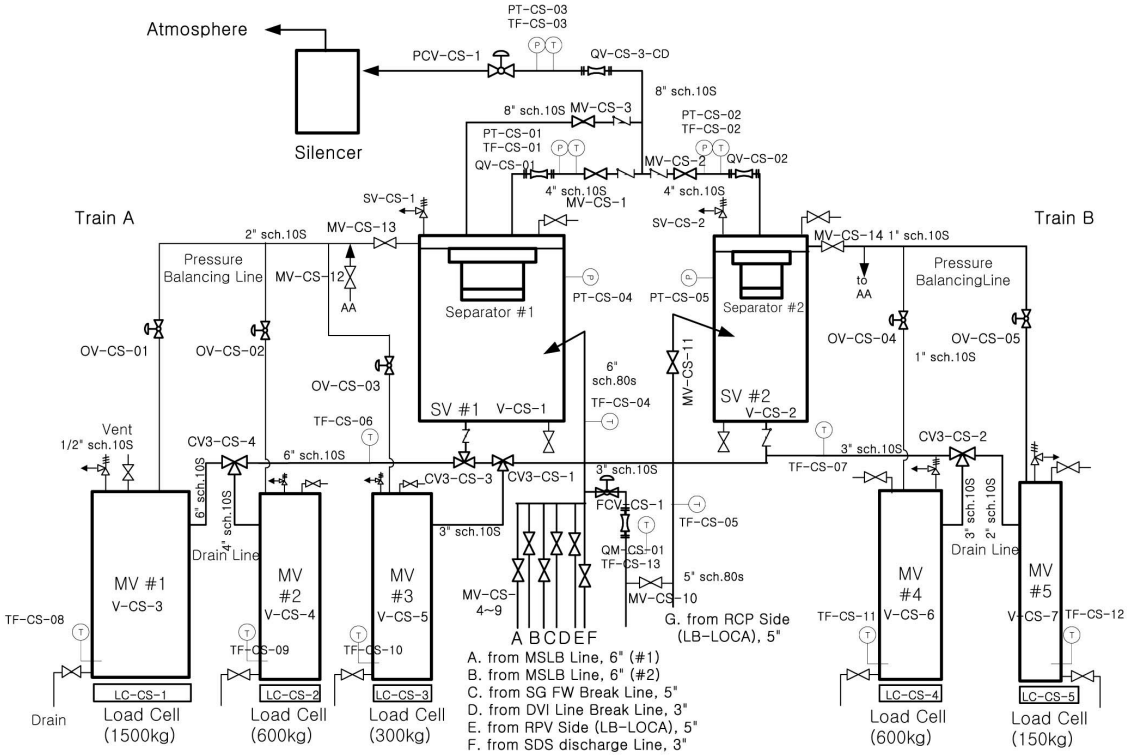

Fig. 3. Schematic Diagram of the Containment Simulation System

containment pressure through pressure regulation. During the present SB-LOCA transient, the measured pressure of the containment simulation tank was used as a boundary condition for the MARS calculation.

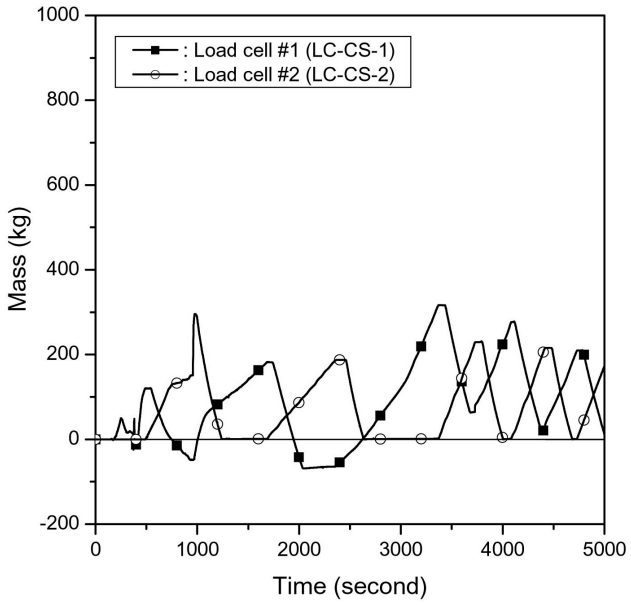

Fig. 4. Measured Load Cell Data During the SB-CL-01 Test

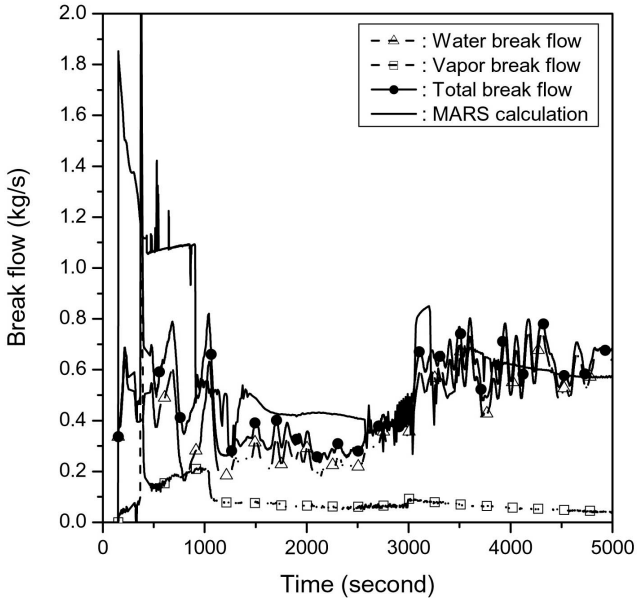

Fig. 5. Comparison of the Break Flow Rate During the SB-CL-01 Test

4.2.2 Core power

Figure 6 shows a core power variation during the present test. The break was started at about 150 seconds. The core power was tripped with a time delay of 88 seconds after the LPP trip signal was generated. When the reactor was tripped, its core power was programmed to follow the power table which had been obtained from the pre-test calculation. Practically, the maximum available core power of the ATLAS was 8% of the scaled power. So, the core power was initially set to be 8% of the scaled power and it was maintained as constant until it intersected with the scaled power curve. Then it was controlled to decay following the scaled power curve. In the post-test calculation, the power curve measured from the present test was used. Figure 6 indicates that the power curve for the post-test calculation was the same as the measured total core power.

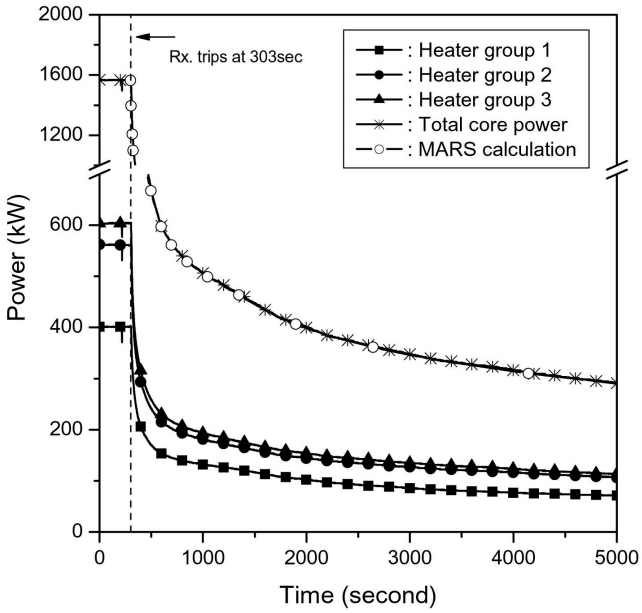

Fig. 6. Comparison of the Core Power During the SB-CL-01 Test

4.2.3 Primary and Secondary Pressures

A comparison of measured trends of primary and secondary pressure after a break is shown in Fig. 7 along with calculation results. Primary pressures were measured at several locations, including the pressurizer, the downcomer, and the upper plenum and lower plenum of the reactor vessel. Among those, the pressure of the upper head plenum is plotted in Fig. 7 as the other pressures do not show any great difference. On initiating

the break, the pressure rapidly dropped until a flashing of the hot coolant started. The primary pressure started to decrease again about 1000 seconds after it was maintained at approximately 9.4MPa in a plateau region. The MARS code generally predicts a similar pressure trend after a break, but the pressure is expected to continuously increase in the observed plateau region. In the present test, the secondary system was isolated at about 221.9 seconds with a time delay after the LPP signal was generated, as shown in Table 3. The feedwater and main steam lines were also simultaneously isolated. The start of the core power trip, however was delayed by 88 seconds to follow the decay curve. During the delay time, the secondary pressure rapidly increased up to the level of the primary pressure due to the energy imbalance. Even though the reactor was tripped at 303 seconds, the primary and the secondary pressures still increased up to 10.7MPa in the MARS calculation. The main cause of the disagreement seems to be due to higher-than-expected heat loss in the ATLAS. After the plateau region, the primary pressure rapidly decreased, but the secondary pressure decreased slowly, maintaining a higher pressure than the primary system during the remaining transient time. In this period, a reverse heat transfer from the secondary system to the primary system in the steam generators was maintained.

At around 3042 seconds, the MARS code also predicts an unobserved peak in the primary pressure. A detailed investigation of the calculation results found that a flow regime inside the U-tubes changes and is either the mist-post-CHF (MPO) or the mist-pre-CHF (MPR) and that a reverse heat transfer rate in a broken steam generator becomes zero at that time. As there is no heat transfer from the secondary side, entrained droplets inside the U-tube pass through the steam generator without evaporation and they are collected in the intermediate legs. A loop seal phenomena in the intermediate leg is inferred to be the main reason for the primary pressure peak. The pressure peak disappears after a short duration, but the intermediate leg is maintained with a sealed condition for a considerable transient time. This loop seal phenomena is also responsible for oscillatory behaviors in the major primary parameters, such as break flow rate, loop flow rate and collapsed water level.

4.2.4 Primary Temperatures

In this test, the hot leg and cold leg temperatures were initially 317 °C and 291 °C, respectively. They are almost similar to the design valves of the APR1400 which are 325 °C and 291 °C, respectively. The hot leg temperature was a little lower than the design value of the APR1400. This was due to a higher primary flow rate than the scaled design value, which was affected by a difficulty in controlling the heat transfer to the secondary side through the steam generators. The ATLAS was

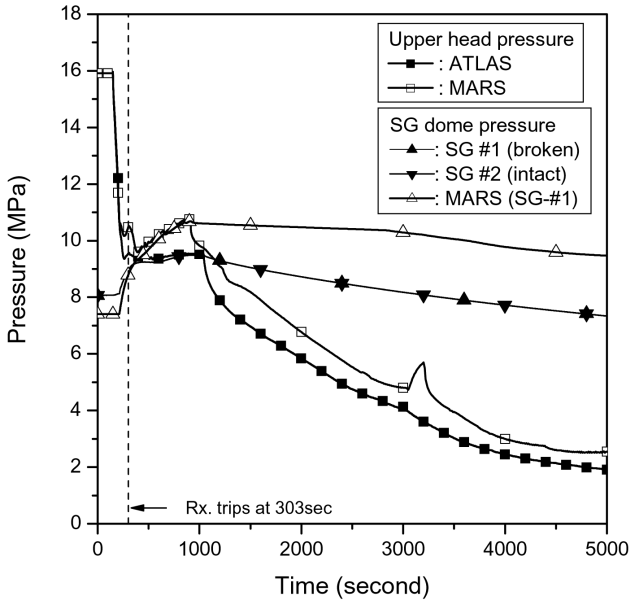

Fig. 7. Comparison of the Primary and Secondary Pressure During the SB-CL-01 Test

designed to have a circulation loop for the secondary system. The steam generated from the steam generators is delivered into the condenser and the condensed water is fed back to the steam generators after reducing its temperature to the design value via a heat exchanger. However, there was great difficulty in controlling the feedwater temperature downstream of the heat exchanger. This was due to the fact that a control valve on the shell side of the heat exchanger was over-designed so we could not control the feedwater temperature properly. The difficulty in controlling the feedwater temperature also resulted in difficulty in controlling the heat transfer to the secondary side through the steam generators. It further affected operator control of the primary coolant flow rate. Consequently, the hot leg temperature was controlled to be lower than the design value by 8 K whereas the cold leg temperature was controlled to be consistent with the design value. In the steady state calculation of the MARS code, the measured hot and cold leg temperatures were used as boundary conditions to obtain the same initial temperature distribution. Another noteworthy observation from the operational viewpoint concerns the effect of the wall structure. The core inlet temperature was observed to be lower than the cold leg temperature by 3 K, as shown in Table 4. This means that the primary coolant was cooled when it passed through the downcomer region, implying that the wall structures of the reactor vessel were insufficiently heated. Thus, the effects of wall structures will have to be carefully assessed in subsequent integral tests.

Figure 8 shows a comparison of the primary temperatures. After the RCPs were tripped at 214 seconds, the hot leg temperature dropped to its saturation temperature and the cold leg temperature increased until the core power was tripped at 303 seconds. Then, the cold leg temperature slowly decreased due to the safety injection flow and then increased to the saturation temperature at around 1040 seconds because of flashing which occurred in the primary system when the primary pressure started to decrease, as shown in Fig.7. The MARS predicts a similar trend to data in the early period of the transient, but the calculated hot leg temperature is higher than the data because the primary pressure was predicted to be higher than the data. Therefore, higher temperature was maintained during the remaining period of the transient. A temperature peak at around 3042 seconds can be explained as having occurred for the same reason described in the previous section.

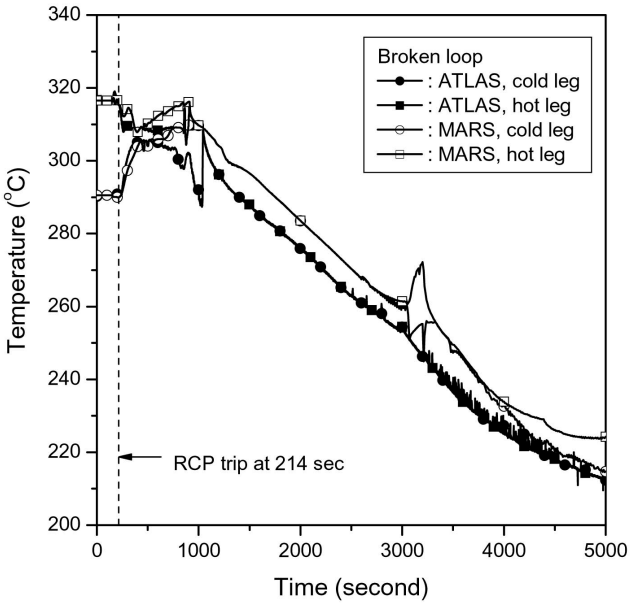

Fig. 8. Comparison of the Primary Temperature During the SB-CL-01 Test

4.2.5 Primary Flow Rate

It is well known that the operation of the RCPs significantly affects the SB-LOCA scenario progression. They may be shut down early during a transient or they may be allowed to run and circulate the coolant through the core for a long time. In the current test, it was assumed that the RCPs stop almost at the same time as the reactor trip. Initially, the RCPs were operated at about 340 rpm to provide the necessary coolant flow rate. Initial steady state conditions require an 8% coolant flow rate to maintain the same temperature difference across the reactor core for a given 8% power. The designed nominal flow rate of the ATLAS RCPs is 25% of the ideally scaled capacity. The 8% core power also provides a natural circulation driving force for circulation of the primary coolant. In the present test, it was found that 340rpm of the RCPs corresponded to the speed necessary to provide an 8% primary coolant flow rate.

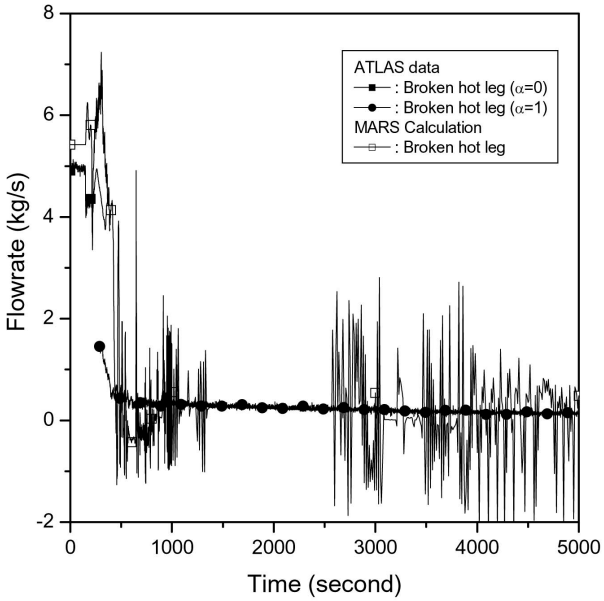

Fig. 9. Comparison of the Primary Flow Rate of the Broken Hot Leg During the SB-CL-01 Test

In order to measure the primary coolant flow rate, a bi-directional flow tube was installed at two hot legs and four cold legs. A bi-directional flow tube can measure bi-directional flow rate in a pipeline from the difference between the dynamic and static pressures, and can also be applicable to a two-phase flow condition if a void fraction at the measuring location is available [14]. A water level measurement transmitter was installed along with the flow tube to obtain a void fraction. The measured flow rates from the two hot legs are plotted in Fig. 9 along with the calculated results. The hot and cold legs of the ATLAS were scaled down to preserve the Froude number according to the local phenomena scaling method. The diameters of the hot and cold legs were determined to be 0.1288m and 0.0873m, respectively. The total length of the hot and cold legs was 1.86m and 1.85m, respectively. Due to the small diameters of the cold and hot legs, it was found that the measured void fraction produced a considerable uncertainty. It seems that the current differential pressure measurement across

the diameter of the legs is not applicable to the fast transient test. A more reliable measurement technique such as a gamma-ray density meter should be utilized in order to obtain a more accurate void fraction in the legs. However, it can be assumed that the flow condition is in a single phase condition full of water in the initial phase of the transient and it becomes a single phase vapor condition during most of the transient time. Accordingly, the measured differential pressure data was post-processed with the assumed void fraction of α=0 or α=1, depending on the transient period. The processed results are plotted in Fig. 9 along with a calculation result. It can be seen in the figure that the MARS code predicts the flow rate in the broken hot leg reasonably well, but that the predicted rate shows a greater oscillatory behavior than the measured data. The oscillation of the primary flow rate seems to be affected by an inventory distribution along the primary piping system. At the moment, the exact pressure loss coefficients along the reactor coolant system are not completely implemented in the code input. Instead, values ideally scaled with respect to the APR1400 were used. This is considered one of the causes for the disagreement between the data and the code prediction.

4.2.6 Primary Collapsed Water Levels

Figure 10 shows the collapsed water level variation of the core normalized with the initial value before a break. It can also be seen from Fig. 10 that the core level gradually decreased and then it remained at a constant value to the end of the test. The collapsed water level in the core was observed to be just below the top of the active core throughout the test period, but no heater rod heat-up was observed because the two-phase mixture level was expected to cover the active core. The prediction of the MARS code for the collapsed water level in the core is generally acceptable. The sudden drop at around 3042 seconds was due to the temporary pressure peak, as shown in the previous section.

Figure 11 shows the collapsed water level variations of the upper head of the reactor pressure vessel, the pressurizer, and the U-tube of the broken steam generator, respectively, normalized with initial values before the break. On initiating the break, the water level in the pressurizer fell rapidly and, with the initiation of a flashing and boiling in the core, a steam volume began to develop in the upper core region. The collapsed water level of the pressurizer was well predicted by the MARS code, but the level of the upper head of the reactor pressure vessel was predicted to decrease faster than the data. This implies that the MARS code predicts much steam generation in the upper head region. It is difficult to explain the cause of this with only the present results, but it seems to be related to a disagreement in the pressure loss coefficients along the pipeline from the upper head to the break system. The MARS code also predicted a response similar to that of the data for the collapsed water level of the broken steam generator. However, the predicted collapsed water level in the U-tube was maintained at about a 20% level during the entire period.

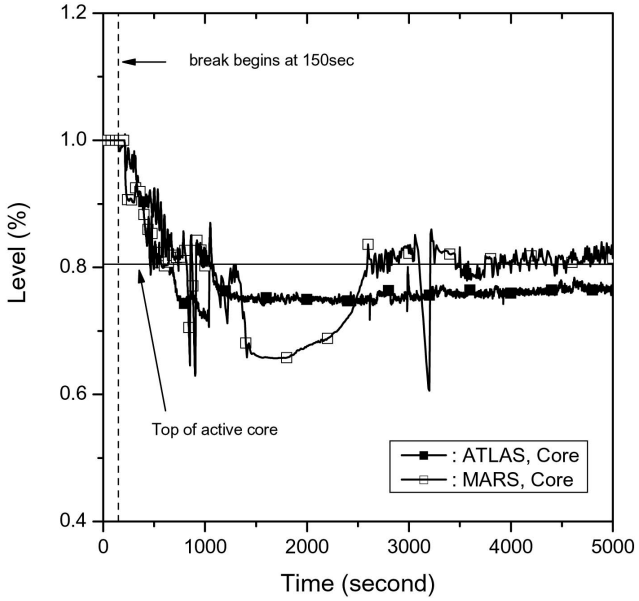

Fig. 10. Comparison of the Normalized Collapsed Water Level of the Core During the SB-CL-01 Test

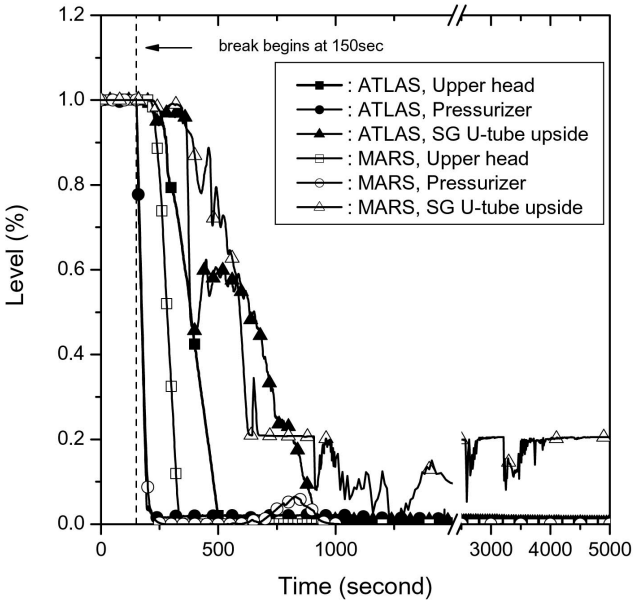

Fig. 11. Comparison of the Normalized Collapsed Water Levels of the Upper Head, the Pressurizer, and the SG U-Tube During the SB-CL-01 Test

The collapsed water levels of the hot and cold legs normalized with their initial values before a break are shown in Figs. 12(a) and 12(b). The calculation results from the MARS code are also plotted for comparison. Only the collapsed water level of the hot leg in a broken loop is plotted in Fig. 12(a) because the other water level in an intact loop showed a similar trend. The water level of the hot leg dropped to about 60% of the hot leg after the LPP signal and showed a gentle oscillation. It dropped to zero at around 1000 seconds for about 1 minute and recovered to its previous level before gradually increasing during the remaining period of the transient. On average, the MARS code predicted a lower collapsed water level than the data. The collapsed water level of the intact cold leg in the broken loop is plotted in Fig. 12(b). The water level also dropped to zero at around 1040 seconds, but then it increased very slowly, which is a different trend from that of the hot leg. The sudden drop in the water level at around 1040 seconds was due to a flashing that occurred when the primary pressure started to decrease again after the plateau period, as can be seen in Fig. 7. In general, the MARS code predicted a trend similar to the data, though it showed some oscillation after 1040 seconds. Such oscillation is closely related to the loop seal phenomena in the intermediate legs.

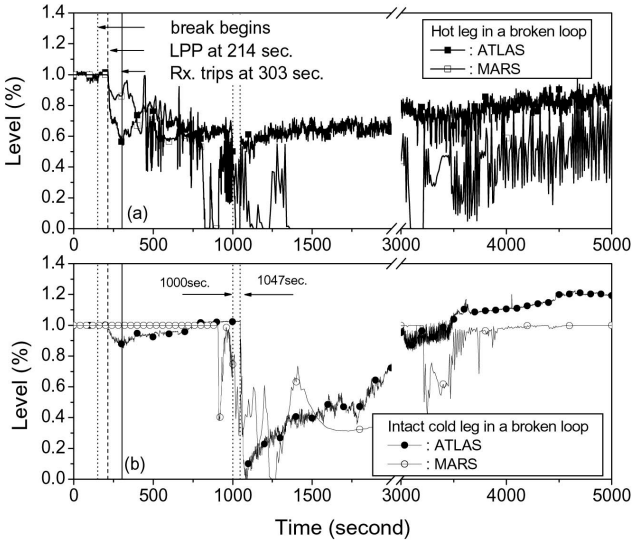

Fig. 12. Comparison of the Normalized Collapsed Levels During the SB-CL-01 Test; (a) Hot Leg (b) Cold Leg

4.2.7 ECC Flows

During SB-CL-01, emergency core cooling water was provided by four SITs and an HPSI pump. As described in the previous section, the speed of the HPSI pump was controlled to deliver a specified flow rate according to a predefined control table. The HPSI pump was started with a time delay of 28.28 seconds after the pressurizer pressure reached the LPP set point. Figure 13 shows the measured HPSI flow rate. During the plateau region of the primary pressure, the HPSI flow rate remained a constant value. When the primary pressure started to decrease at around 1000 seconds, the HPSI flow rate increased according to the control table. The SIT was started by opening the isolation valves connected to the primary system when the primary pressure reached 4.03MPa. However, the SIT flow rate showed a large fluctuation, so it was very difficult to identify the resultant flow rate. We found that the calibration of the SIT flow meter was done with a much higher measurement range. To be consistent with the data, the measured HPSI flow rate was used as a boundary condition in the MARS calculation. It can be seen from Fig.13 that the predicted trend is reasonably consistent with the data.

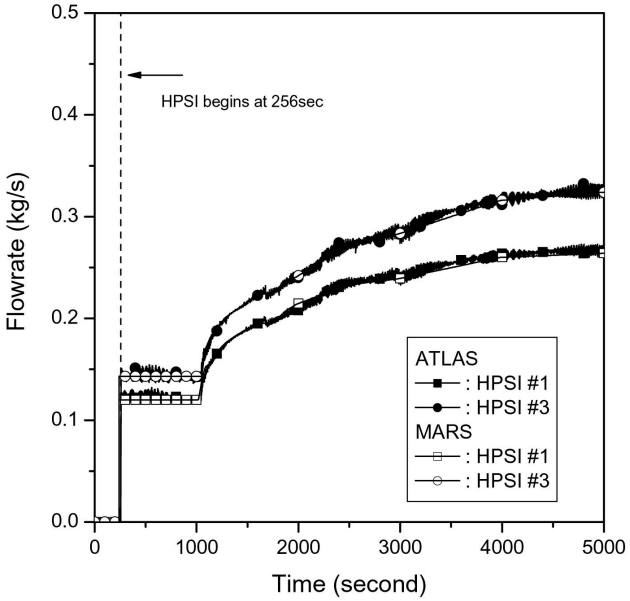

Fig. 13. Comparison of the HPSI Flow Rate During the SB-CL-01 Test

5. CONCLUSIONS

The ATLAS is a vast and complex test facility, consisting of many fluid sub-systems and instrumentation and control systems. The present work is the first integral effect test to verify the performance of all the sub-systems of the ATLAS and to identify systems which require further design improvement. A preliminary SB-LOCA with a break size equivalent to a 3-inch cold leg break of the APR1400 was performed. Reasonably good thermal hydraulic data

was obtained so that an integral performance of the fluid sub-systems was identified and control performance of the ATLAS was confirmed under real thermal hydraulic conditions. It was shown that the major devices were well controlled and followed the pre-calculated sequence of events. A few components or systems which require further design improvement were identified during the course of testing, including the measurement techniques of the bi-directional flow meter, the break flow measuring system, and the heat exchanger design in the secondary system, etc. The present findings will contribute to enhancing the simulation capability of the ATLAS for a broad range of target scenarios.

Based on the obtained data, a post-test calculation was carried out with the best estimate thermal hydraulic system analysis code, MARS 3.1. In general, the predictions showed good agreement with the measured data, though some disagreements were found. One of the main causes of the disagreements is inferred to be the mismatch in pressure loss coefficients along the reactor coolant system. A future study will use the present data to improve the input model for the MARS code in order to better reflect the real system characteristics of the ATLAS.

ACKNOWLEDGMENTS

The authors would like to thank the Korean Ministry of Science and Technology for their financial support of the Nuclear R&D Program.

REFERENCES

[1] S. K. Moon, C.-H. Song, C. K. Park, T. S. Kwon, B. J. Yun and M. K. Chung, "A state-of-the-Art Report on the Study of the Nuclear Reactor Thermal Hydraulics Using Integral Test Facilities," KAERI/AR-509/98 (1998).

[2] Y. S. Kim, B. U. Bae, and G. C. Park, "Integral Loop Test and Assessment of Modified RELAP5/MOD3.3 for RCS Coolant Inventory during a LBLOCA," *Nuclear Engineering and Design*, **237**, 182 (2007).

[3] B. U. Bae, K. H. Lee, and G. C. Park, "Integral Experiment and RELAP5 Analysis for DVI line Break SBLOCA in APR1400," ICAPP '07, Nice, France, May 13-18 (2007).

[4] W. P. Baek, C.-H. Song, B. J. Yun, T. S. Kwon, S. K. Moon and S. J. Lee, "KAERI Integral Effect Test Program and the ATLAS Design," *Nucl. Technol.*, **152**, 183 (2005).

[5] K. Y. Choi, H. S. Park, D. J. Euh, T. S. Kwon, and W. P. Baek, "Simulation Capability of the ATLAS Facility for Major Design-Basis Accidents," *Nucl. Technol.*, **156**, 256 (2006).

[6] I. C. Chu, C.-H. Song, B. H. Cho and J. K. Park, "Development of Passive Flow Controlling Safety Injection Tank for APR1400," *Nuclear Engineering and Design*, **238**, 200 (2007).

[7] Y. S. Kim, W. P. Baek, C.-H. Song, K. Y. Choi, H. S. Park, S. Cho, K. H. Kang, B. D. Kim, S. K. Moon, B. J. Yun, C. H. Chung, T. S. Kwon, D. J. Euh, N. H. Choi, J. K. Park, and K. H. Min, "Startup Test Report of ATLAS," KAERI/TR-3330/2007 (2007).

[8] "MARS Code Manual Volume I: Code Structure, System Models, and Solution Methods," KAERI/TR-2812/2004 (2004).

[9] M. Ishii and I. Kataoka, "Similarity Analysis and Scaling Criteria for LWRs Under Single Phase and Two-Phase Natural Circulation," NUREG/CR-3267, ANL-83-32, Argonne National Laboratory (1983).

[10] H. S. Park, S. K. Moon, B. J. Yun, T. S. Kwon, K. Y. Choi, C. K. Park, S. Cho, S. D. Hong, S. J. Yi, Y. S. Kim, C.-H. Song, and W. P. Baek, "Calculation Sheet for the Basic Design of the ATLAS Fluid System," KAERI/TR-3333/2007 (2007).

[11] K. Y. Choi, T. S. Kwon, S. Cho, H. S. Park, J. T. Kim and W. P. Baek, "Control and Data Acquisition System of the ATLAS Facility," KAERI/TR-3338/2007 (2007).

[12] INEL, "RELAP5/MOD3.2.1 Code Manual," USNRC Report, NUREG/CR-5535 (1998).

[13] M.J. Thurgood and M. J. George, "COBRA/TRAC: A Thermal-hydraulics Code for Transient Analysis of Nuclear Reactor Vessels and Primary Coolant Systems," USNRC Report, NUREG/CR-3046 (1983).

[14] B. J. Yun, D. J. Euh, K. H. Kang, C.-H. Song, and W. P. Baek, "Development of an Average Bidirectional Flow Tube for a Measurement of the Single and Two Phase Flow," The 11th Int. Topical Meeting on Nuclear Reactor Thermal-Hydraulics (NURETH-11), Avignon, France, October 2-6 (2005).